Bulletin of the Seismological Society of America, Vol. 104, No. 5, pp. –, October 2014, doi: 10.1785/0120140077

Short Note

Phase-Weighted Stacking Applied to Low-Frequency Earthquakes

by Clifford H. Thurber, Xiangfang Zeng, Amanda M. Thomas,* and Pascal Audet

Abstract We apply phase-weighted stacking (PWS) to the analysis of low-frequency earthquakes (LFEs) in the Parkfield, California, region and central Cascadia. The technique uses the coherence of the instantaneous phase among the stacked signals to enhance the signal-to-noise ratio (SNR) of the stack. We find that for picking LFE arrivals for the Parkfield, California, region and for LFE template formation in central Cascadia, PWS is extremely effective. For LFEs in the Parkfield, California, region, PWS yields many more usable phases than standard linear stacking; and, for LFE detection in Cascadia, PWS produces templates with much higher SNR than linear stacking.

Introduction

Waveform cross correlation and stacking has become an increasingly valuable tool for a broad class of seismic analysis techniques. Among the most prevalent is the extraction of empirical Green's functions for wave propagation between station pairs using ambient noise cross correlation (ANCC; see Campillo, 2014, and references therein). Although the basic approach for ANCC is well established (Bensen *et al.*, 2007; Snieder and Wapenaar, 2010), methods for improving the technique are continually being sought. A particularly promising strategy for improvement is phase-weighted stacking, or PWS (Schimmel and Paulssen, 1997). The PWS method has been further extended by Schimmel and Gallart (2007) to use frequency-dependent time windowing, employing the S transform. They term their modified method "time–frequency-PWS," or tf-PWS. PWS and tf-PWS have been shown to be effective for enhancement of signal extraction for body-wave and surface-wave Green's functions from ambient noise (Baig *et al.*, 2009; Schimmel *et al.*, 2011). We explore the utility of PWS for enhancing the stacking of low-frequency earthquakes (LFEs) beneath the San Andreas fault near Parkfield, California, and for detection of LFEs via network cross correlation in central Cascadia. We find that PWS is remarkably effective for reducing noise in LFE stacks, improving the quality of what previously were reasonably good stacks, and making many previously poor stacks usable.

Phase-Weighted Stacking Method

Following the general notation of Schimmel and Paulssen (1997), the standard linear stack $g_{\mathrm{ls}}(t)$ simply averages the N constituent traces (signals) $s_i(t)$:

$$g_{\mathrm{ls}}(t) = \frac{1}{N}\sum_{j=1}^{N} s_j(t). \qquad (1)$$

The basic idea underlying PWS is to down weight components of signals in a stack that do not share the same instantaneous phase. Thus, coherent components of waveforms dominate the contribution to the stack, markedly reducing the effect of incoherent noise. Schimmel and Paulssen (1997) describe an effective approach for accomplishing this goal. Closely following their notation, each trace $s_j(t)$ and its Hilbert transform $\mathrm{H}[s_j(t)]$ are combined to form the complex trace (analytic signal) $S_j(t)$

$$S_j(t) = s_j(t) + i\,\mathrm{H}[s_j(t)], \qquad (2)$$

which can be rewritten in terms of amplitude $A(t)$ and instantaneous phase $\Phi_j(t)$ as

$$S_j(t) = A_j(t)\exp[i\Phi_j(t)]. \qquad (3)$$

Schimmel and Paulssen (1997) define the phase stack $c(t)$ as

$$c(t) = \frac{1}{N}\sum_{j=1}^{N}\exp[i\Phi_j(t)]. \qquad (4)$$

If the instantaneous phase is exactly the same for all traces in the stack at time t, the corresponding value of c will be 1 (Fig. 1a). If the instantaneous phase varies somewhat from trace to trace, c will be less than 1 (Fig. 1b). If the instantaneous phase varies quite randomly, c will be approximately 0 (Fig. 1c). Thus, weighting the waveform stack by $[c(t)]^{\nu}$ will tend to suppress incoherent signals, that is, signals that are not in phase. The exponent ν controls the fall-off of the

*Also at Department of Geological Sciences, University of Oregon, Eugene, Oregon 97403

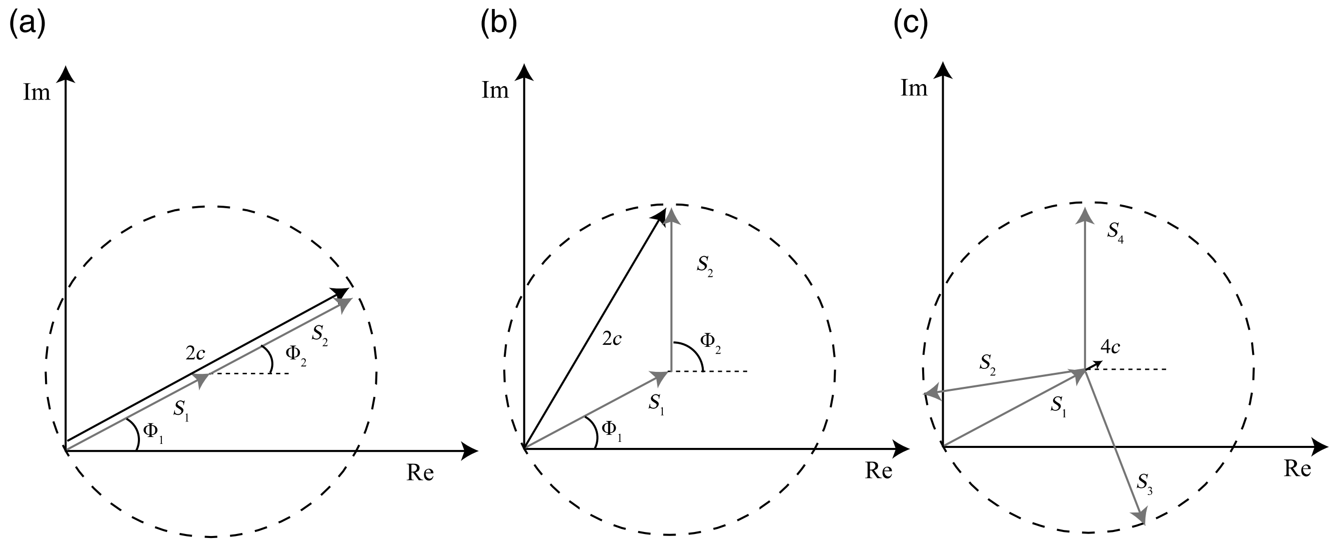

Figure 1. (a) When two signals have the same instantaneous phase, the phase sum will be 2 and the corresponding value of c will be 1. (b) When the instantaneous phase varies somewhat from trace to trace, the phase sum will be less than 2 and c will be less than 1. (c) When the instantaneous phase varies quite randomly, the phase sum and c will both be approximately 0. After Schimmel and Paulssen (1997).

contribution of each sample to the stack with decreasing value of c. We note that coherency weighting has also been utilized for improving waveform alignment via cross correlation (Rowe *et al.*, 2002), but to our knowledge it has not previously been applied to LFE stacking.

Schimmel and Paulssen (1997) demonstrate the effectiveness of PWS on synthetic and real data for seismic arrays, using $\nu = 2$. They also compare PWS to other techniques, including the energy-normalized cross-correlation sum (Neidell and Taner, 1971), the coherency functional (Gelchinsky *et al.*, 1985), and semblance (Taner and Koehler, 1969; Neidell and Taner, 1971). Schimmel and Paulssen (1997) emphasize the point that, unlike these other methods, PWS applies no penalty for varying signal amplitude. This can be advantageous in some circumstances, such as for weak arrivals. However, PWS does not preserve amplitude, so that can be a drawback for some applications.

The tf-PWS method is an extension of PWS that uses an S-transform decomposition (Schimmel and Gallart, 2007),

$$S(\tau, f) = \int_{-\infty}^{\infty} u(t) w(\tau - t, f) e^{-i2\pi f t}, \qquad (5)$$

with a Gaussian window function w given by

$$w(\tau - t, f) = \frac{|f|}{k\sqrt{2\pi}} \exp\{[-f^2(\tau - t)^2]/(2k^2)\}, \qquad k > 0. \qquad (6)$$

Under certain conditions, the S transform provides an analytic representation of a real signal. Schimmel and Gallart (2007) use the phase coherence $C_{\text{ps}}(\tau, f)$ to enhance the coherent part of the signal of the linear stack in the time–frequency domain such that

$$C_{\text{ps}}(\tau, f) = \left| \frac{1}{N} \sum_{j=1}^{N} \frac{S_j(\tau, f) e^{i2\pi f \tau}}{|S_j(\tau, f)|} \right|^{\nu}, \qquad (7)$$

in which the denominator is the real part of $S_j(\tau, f)$, and $S_j(\tau, f)$ denotes the S transform of the jth trace. The tf-PWS trace is obtained as the inverse S transform of the C_{ps}-weighted summation of the S transform of each trace:

$$S_{\text{tf-pws}}(t) = \text{inv}\{C_{\text{ps}}(\tau, f) S_{\text{linear}}(\tau, f)\}. \qquad (8)$$

We demonstrate the utility of tf-PWS and PWS for enhancing LFE signals in Parkfield, California, and central Cascadia, respectively.

Application to LFEs in Parkfield, California

To evaluate the performance of tf-PWS for individual LFE arrivals, we analyzed records of LFE families identified by Shelly and Hardebeck (2010) and recorded by the Parkfield Area Seismic Observatory (PASO). One (family 18319) is to the northwest of Parkfield on the edge of the PASO array, and the other (family 35503) is close to Cholame, about 40 km southeast of the PASO array (Fig. 2). We selected two LFE families outside the PASO array to illustrate the improvement possible for lower signal-to-noise ratio (SNR) cases. For the first family, we have PASO data for 19 LFEs that occurred between 2001 and 2002. Using a 20 s time window beginning 5 s before the origin time, the raw three-component data in selected time windows were stacked with linear stacking and tf-PWS. In linear stacking, the weight of each trace is equal. Figure 3a shows high-pass filtered (corner frequency of 1 Hz) stacked traces. For stations POND and POWR, the phases of the LFE signal for both linear and tf-PWS stacks are

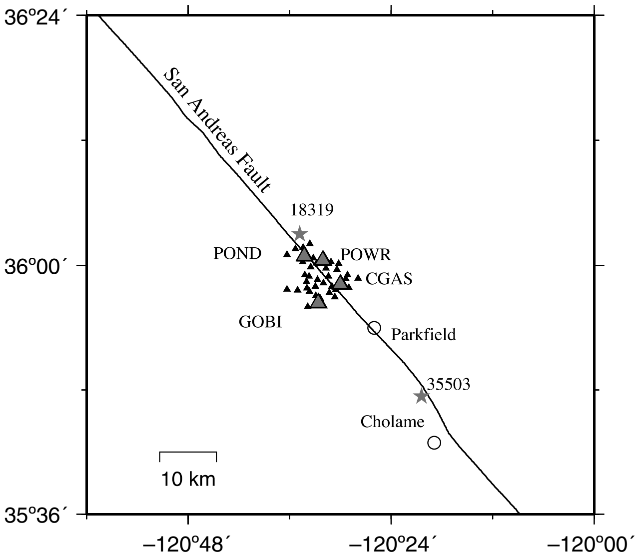

Figure 2. Location of the Parkfield Area Seismic Observatory (PASO) stations (four-letter station name codes) and low-frequency earthquake (LFE) families (five-digit family numbers) analyzed with time–frequency phase-weighted stacking (tf-PWS).

consistent, but the noise has been significantly suppressed in the tf-PWS stack. For stations CGAS and GOBI, the tf-PWS stack yields phases that could not be picked in the linear stacks. For family 35503 (Fig. 3b), only the POWR linear stack produced usable phases, but tf-PWS yields good quality phases for all stations. The mean increase in SNR for the tf-PWS stacks relative to the linear stacks is a factor of 2.1 for family 18319 and a factor of 3.0 for family 35503. These examples show that tf-PWS has significant potential for improving the SNR for LFEs in order to enhance phase picking.

Application to LFEs in Cascadia

In addition to the utility of PWS in improving individual arrivals, the overall improvement in template quality is important when attempting LFE detection via network cross correlations in environments with poor station coverage or data quality. LFE templates have been identified using visual identification (Shelly *et al.*, 2006; Frank *et al.*, 2013), autocorrelation (Brown *et al.*, 2008; Brown *et al.*, 2009; Tang *et al.*, 2010; Bostock *et al.*, 2012; Royer and Bostock, 2014),

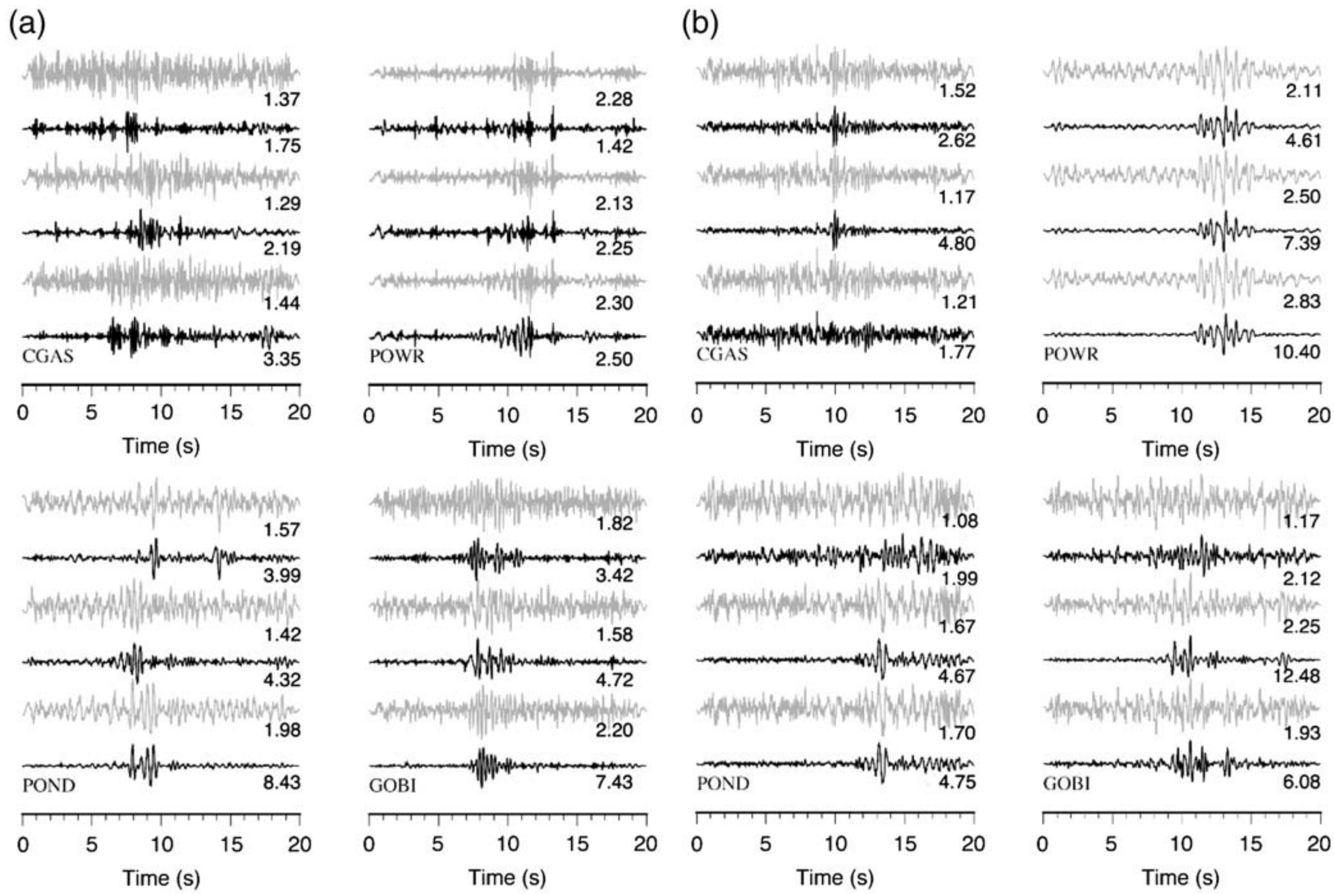

Figure 3. (a) Stacked traces of LFE family 18319 at stations CGAS, POWR, POND, and GOBI. (b) Stacked traces of LFE family 35503 at stations CGAS, POWR, POND, and GOBI. The gray and black traces denote the linear and tf-PWS stacks, respectively. From top to bottom, the vertical, north, and east components are plotted in each panel, along with signal-to-noise ratio (SNR) values.

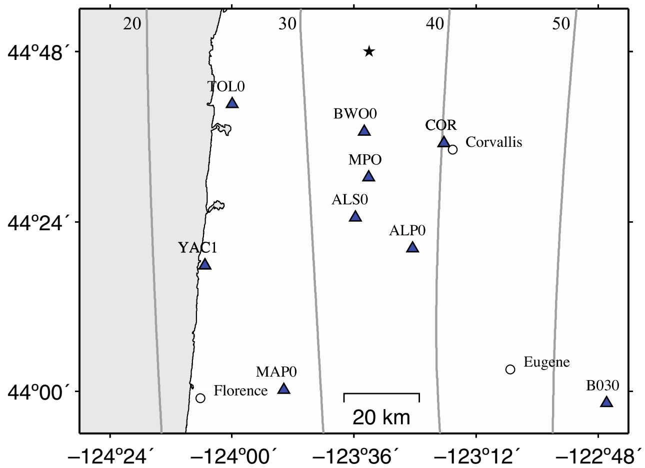

Figure 4. Cascadia stations (triangles) and LFE locations (star). The color version of this figure is available only in the electronic edition.

subspace detection (Maceira *et al.*, 2010), and cross-station methods (Rubin and Armbruster, 2013). Once templates are identified, LFE detections are registered using network cross correlation whereby templates are cross correlated through continuous network data to register additional detections (defined as times when the summed cross correlation exceeds some threshold, typically eight times the median absolute deviation), and those detections are stacked to create a new template with a better SNR (Gibbons and Ringdal, 2006). This process is iterated until the incorporation of additional detections no longer improves template quality.

To demonstrate the utility of PWS in LFE detection using network cross correlation, we use data from central Oregon during the 2009 episodic tremor and slip event (Fig. 4). We note that the closest stations to the north had insufficient SNR to yield useful stacks, so we focused on stations to the south. Data were band-pass filtered between 1 and 8 Hz and resampled to 40 samples/s. Though prevalent tremor exists throughout central Oregon (Wech and Creager, 2008), identification of templates via autocorrelation methods systematically fails due to sparse station coverage, low SNR of many stations, and the paucity of individual LFEs (i.e., LFEs generally occur as swarms of events in rapid succession). Candidate LFE templates were identified using the method of Savard and Bostock (2013), which is a cross-station approach similar to that of Rubin and Armbruster (2013). We then use the iterative network cross-correlation procedure described above to register additional detections in a three-day window and further refine the LFE templates.

Figure 5 shows the evolution of one LFE template over five iterations using both linear stacking and PWS. Using linear stacking, a total of 169, 505, and 802 LFEs are registered after iterations 1, 3, and 5, respectively. Although the total number of detections is approximately the same after five iterations using PWS (it is approximately 10% higher), the result is a cleaner template with abrupt *P*- and *S*-wave onsets, clearly identifiable *S*-wave moveout on stations to the south

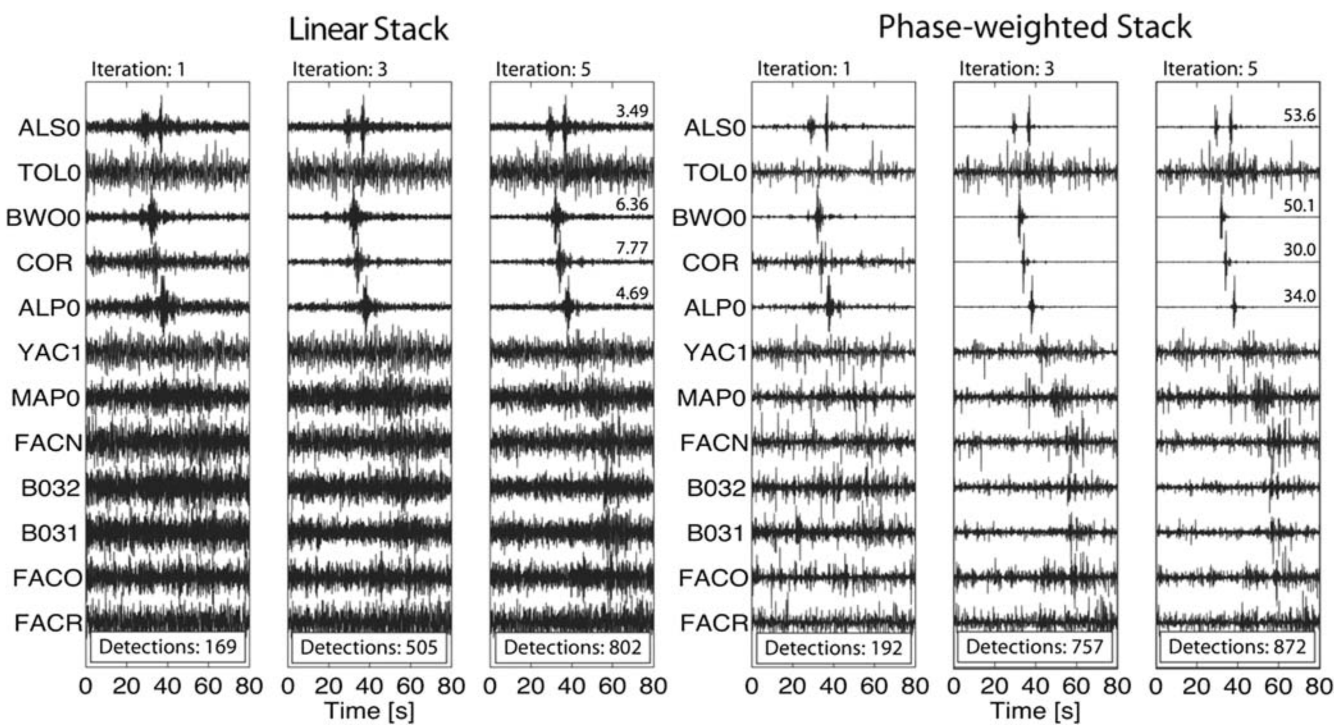

Figure 5. LFE template evolution over five iterations using linear stacking and PWS. Each panel shows horizontal-component seismograms for stations in central Oregon. The iteration and number of detections are annotated in each panel. In this particular case, the total number of detections is similar after five iterations; however, the use of PWS results in a cleaner template with higher SNR than the linear stack, as indicated in the panels of iteration 5.

(e.g., MAP0, FACN, B032), and higher SNRs. The mean increase in SNR for the tf-PWS stacks relative to the linear stacks is a factor of 8.6. The results are similar for other LFE families in central Oregon and in northern California, where data quality is comparable. These results suggest that incorporating PWS into iterative network cross-correlation approaches improves the overall template quality and may increase the number of LFE detections.

Summary

The application of weighting reflecting the phase coherence of the signals when stacking LFE traces yields substantial improvement in SNR in the stacked traces. For LFEs in the Parkfield, California, region, tf-PWS yields many more usable phases than does standard linear stacking. Similarly, for LFE detection in Cascadia, PWS produces templates with much higher SNR than linear stacking. Our experience suggests that PWS and tf-PWS will be extremely useful for LFE studies in other regions.

Data and Resources

Seismograms from the Parkfield region used in this study were collected as part of the Parkfield Area Seismic Observatory experiment using Program for Array Seismic Studies of the Continental Lithosphere (PASSCAL) instruments. Data can be obtained from the Incorporated Research Institutions for Seismology Data Management Center (IRIS-DMC) at www.iris.edu (last accessed January 2014). Central Cascadia waveforms are a combination of data collected from the Plate Boundary Observatory borehole network, the Pacific Northwest Seismic Network, and the Flexarray Along Cascadia Experiment for Segmentation experiment. Data were downloaded from the IRIS-DMC at www.iris.edu (last accessed January 2013).

Acknowledgments

We thank Associate Editor Cezar Trifu and two anonymous reviewers for their constructive comments and David Shelly for assistance with the Parkfield LFEs. This work was supported by the National Earthquake Hazards Reduction Program, under U.S. Geological Survey (USGS) Award G14AP00056. The views and conclusions contained in this document are those of the authors and should not be interpreted as necessarily representing the official policies, either expressed or implied, of the U.S. Government. This research was also supported by the Southern California Earthquake Center (SCEC). SCEC is funded by National Science Foundation (NSF) Cooperative Agreement EAR-1033462 and USGS Cooperative Agreement G12AC20038. The SCEC contribution number for this paper is 1954. A. M. T. gratefully acknowledges support from National Science Foundation Postdoctoral Fellowship EAR-1249775. P. A. acknowledges funding from the Natural Science and Engineering Research Council of Canada.

References

Baig, A. M., M. Campillo, and F. Brenguier (2009). Denoising seismic noise cross correlations, *J. Geophys. Res.* **114,** no. B08310, doi: 10.1029/2008JB006085.

Bensen, G. D., M. H. Ritzwoller, M. P. Barmin, A. L. Levshin, F. Lin, M. P. Moschetti, N. M. Shapiro, and Y. Yang (2007). Processing seismic ambient noise data to obtain reliable broadband surface wave dispersion measurements, *Geophys. J. Int.* **169,** 1239–1260, doi: 10.1111/j.1365-246X.2007.03374.x.

Bostock, M. G., A. A. Royer, E. H. Hearn, and S. M. Peacock (2012). Low frequency earthquakes below southern Vancouver Island, *Geochem. Geophys. Geosyst.* **13,** Q11007, doi: 10.1029/2012GC004391.

Brown, J. R., G. C. Beroza, S. Ide, K. Ohta, D. R. Shelly, S. Y. Schwartz, W. Rabbel, M. Thorwart, and H. Kao (2009). Deep low-frequency earthquakes in tremor localize to the plate interface in multiple subduction zones, *Geophys. Res. Lett.* **36,** L19306, doi: 10.1029/2009GL040027.

Brown, J. R., G. C. Beroza, and D. R. Shelly (2008). An autocorrelation method to detect low frequency earthquakes within tremor, *Geophys. Res. Lett.* **35,** L16305, doi: 10.1029/2008GL034560.

Campillo, M. (2014). Noise correlations, in *Treatise on Geophysics*, Second Ed., G. Schubert (Editor), Vol. 1, Elsevier Ltd., Amsterdam, The Netherlands.

Frank, W. B., N. M. Shapiro, V. Kostoglodov, A. L. Husker, M. Campillo, J. S. Payero, and G. A. Prieto (2013). Low-frequency earthquakes in the Mexican sweet spot, *Geophys. Res. Lett.* **40,** 2661–2666, doi: 10.1002/grl.50561.

Gelchinsky, B., E. Landa, and V. Shtivelman (1985). Algorithms of phase and group correlation, *Geophysics* **50,** 596–608.

Gibbons, S. J., and F. Ringdal (2006). The detection of low magnitude seismic events using array-based waveform correlation, *Geophys. J. Int.* **165,** 149–166, doi: 10.1111/j.1365-246X.2006.02865.x.

Maceira, M., C. A. Rowe, G. Beroza, and D. Anderson (2010). Identification of low-frequency earthquakes in non-volcanic tremor using the subspace detector method, *Geophys. Res. Lett.* **37,** L06303, doi: 10.1029/2009GL041876.

Neidell, N. S., and M. T. Taner (1971). Semblance and other coherency measures for multi-channel data, *Geophysics* **36,** 482–497.

Rowe, C. A., R. C. Aster, B. Borchers, and C. J. Young (2002). An automatic, adaptive algorithm for refining phase picks in large seismic data sets, *Bull. Seismol. Soc. Am.* **92,** 1660–1674.

Royer, A. A., and M. G. Bostock (2014). A comparative study of low frequency earthquake templates in northern Cascadia, *Earth Planet. Sci. Lett.* doi: 10.1016/j.epsl.2013.08.040, ISSN: 0012821X.

Rubin, A. M., and J. G. Armbruster (2013). Imaging slow slip fronts in Cascadia with high precision cross-station tremor locations, *Geochem. Geophys. Geosyst.* **14,** 5371–5392, doi: 10.1002/2013GC005031.

Savard, G., and M. G. Bostock (2013). Detection and location of low frequency earthquakes using cross-station correlation, presented at 2013 Fall *Meeting, American Geophysical Union*, San Francisco, California, Abstract S41B–2436.

Schimmel, M., and J. Gallart (2007). Frequency-dependent phase coherence for noise suppression in seismic array data, *J. Geophys. Res.* **112,** no. B04303, doi: 10.1029/2006JB004680.

Schimmel, M., and H. Paulssen (1997). Noise reduction and detection of weak, coherent signals through phase-weighted stacks, *Geophys. J. Int.* **130,** 497–505, doi: 10.1111/j.1365-246X.1997.tb05664.x.

Schimmel, M., E. Stutzmann, and J. Gallart (2011). Using instantaneous phase coherence for signal extraction from ambient noise data at a local to a global scale, *Geophys. J. Int.* **184,** 494–506, doi: 10.1111/j.1365-246X.2010.04861.x.

Shelly, D. R., and J. L. Hardebeck (2010). Precise tremor source locations and amplitude variations along the lower-crustal central San Andreas Fault, *Geophys. Res. Lett.* **37,** L14301, doi: 10.1029/2010GL043672.

Shelly, D. R., G. C. Beroza, S. Ide, and S. Nakamula (2006). Low-frequency earthquakes in Shikoku, Japan and their relationship to episodic tremor and slip, *Nature* **442,** 188–191.

Snieder, R., and K. Wapenaar (2010). Imaging with ambient noise, *Phys. Today* **63,** 44–49.

Taner, M. T., and F. Koehler (1969). Velocity spectra—Digital computer derivation and applications of velocity functions, *Geophysics* **34,** 859–881.

Tang, C.-C., Z. Peng, K. Chao, C.-H. Chen, and C.-H. Lin (2010). Detecting low-frequency earthquakes within non-volcanic tremor in southern Taiwan triggered by the 2005 M_w 8.6 Nias earthquake, *Geophys. Res. Lett.* **37,** L16307, doi: 10.1029/2010GL043918.

Wech, A. G., and K. C. Creager (2008). Automated detection and location of Cascadia tremor, *Geophys. Res. Lett.* **35,** L20302, doi: 10.1029/2008GL035458.

Department of Geoscience
University of Wisconsin-Madison
Madison, Wisconsin 53706
(C.H.T., X.Z.)

Department of Geophysics
Stanford University
397 Panama Mall
Stanford, California 94305
(A.M.T.)

Department of Earth Sciences
University of Ottawa
140 Louis Pasteur
Ottawa, Canada ON K1N 6N5
(P.A.)

Manuscript received 26 March 2014;
Published Online 19 August 2014